A Singular Value Decomposition Model for MIMO Channels at 2.6GHz

Yang Liu Ye Wang Wen-jun Lu Hong-bo Zhu
Nanjing University of Posts and Telecommunications
Nanjing,Jiangsu Province,China
ly71354@163.com

***Abstract*- A novel MIMO model based on singular value decomposition of matrix is proposed in this paper. A corridor to stair MIMO measurement at 2.6GHz is conducted in order to evaluate the performance of the novel model. The joint DoA-DoD-delay power spectrum and the channel capacity of the model are compared with those obtained from the measured channels. The results show clearly that the joint DoA-DoD-delay power spectrum and the channel capacity of the novel model provides a better fit to the measured data than other models.**

I. Introduction

LTE(Long Term Evolution), as one of the key technologies for 4G wireless communication systems, has been put forward to support high rates and large capacity gains. For LTE system, the use of MIMO(Multiple-Input Multiple-Output) combined with OFDM(orthogonal-frequency multiple access) is the most promising strategy[1]. In China, the allocation spectra for indoor LTE wireless communication system is from 2.5 GHz to 2.69 GHz. Accurate MIMO channel model is an important tool to enhance the performance of LTE wireless communication system. In the past years, several MIMO channel models have been proposed. They can be classified into physical models and analytical models [2,3]. Physical models describing electromagnetic wave propagation environment are independent of the antenna configuration. Saleh-Valenzuela model [4,5], Zwick model [6], geometry-based stochastic model(GSCM) [7] are three typical physical models. On the other hand, analytical models considering antenna array configuration are often used to describe the channel impulse response(CIR) matrix.

Among all the analytical models, Kronecker model [8], Weichselberger model [9] and virtual channel representation model [10] are the most typical models. Kronecker model based on the assumption that the spatial correlation coefficient at the transmitter (receiver) is independent of receiver (transmitter). That is to say the one-sided spatial correlation matrix of transmitter (receiver) is independent of receiver (transmitter). It is confirmed that this assumption is in general too strict for channel by realistic channel measurements. Different with Kronecker model, Weichselberger model is based on the assumption that the eigenbases of one-sided spatial correlation matrix at the transmitter (receiver) depend on the environment, i.e., number of antennas, positions, and scatterers. However, it is shown that this assumption holds only approximately and the eigenbases are also influenced by the spatial structure of transmit signals in [11]. In [10], Sayeed develops a virtual channel representation model that the eigenbases at the transmitter and receiver in Weichselberger model are replaced by the steering matrices into the virtual angles at the transmitter and receiver respectively. The virtual channel representation model is only available for uniform linear arrays (ULAs) and spatial resolution of the model deponds on the antenna array size.

In this paper ,a novel MIMO channel model is presented based on the singular value decomposition (SVD) of matrix. Measurement setup and environment are described in Part Ⅱ. In Part Ⅲ, a novel MIMO model based on the singular value decomposition of matrix is established. In Part Ⅳ, measured results and model results are shown to evaluate the performance of the novel model.

Throughout the paper, we will use the vec(·) operator that stacks the columns of a matrix into one vector. The superscripts $[\cdot]^H$, $[\cdot]^T$, $[\cdot]^*$ stands for complex conjugate matrix transpose operator, matrix transpose operator, and complex conjugate operator, respectively. The symble ⊗ stands for the Kronecker product of two matrices. Finally, E(·) denotes the expectation operator.

II. Measurement Setup

A. Measurement System

Fig.1 shows a 2×2 MIMO measurement system conducted by Agilent 8753ES vector network analyzer (VNA). The VNA generates a 20MHz swept signal at a center frequency of 2.6GHz. The transmitted power is 10 dBm. The transmit and

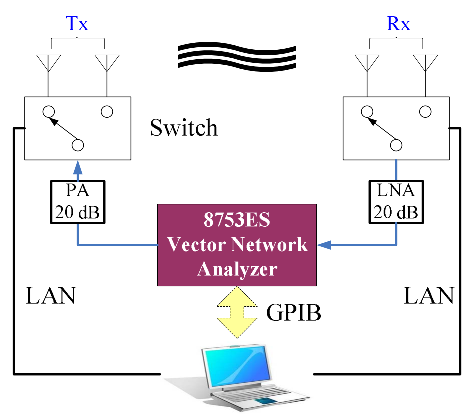

Figure 1: block diagram of MIMO measurement system.

This work was supported by National Science and Technology Major Project under granted no. 2012ZX03001028-005 and 2011ZX03005-004-03 and Jiangsu 973 project (BK2011027).

receive antennas are the same omnidirectional monopoles with a gain of 3 dBi. Transmit and receive antennas are connected to Agilent 34980A switch matrix respectively. The transmit signal is amplified by a 20dB power amplifier. The receive signal is amplified by a 20dB low noise power amplifier and conducted to the VNA via 20 meters coaxial cable. A lap top is used to sample the measured data through GPIB interface and control the switch matrix via LAN. The measurement is carried out without moving persons to make sure of the time-invariant channel behavior during one snapshot, which is about 20 seconds. We conduct measurement according to the transmit antenna spacing and receive antenna spacing as 0.5λ, 1λ, 2λ respectively, where λ is wavelength.

B. Environment

As shown in Fig.2, the measurement environment is in an office building that contains a 15m corridor to a stair through a corner. This paper discusses not line of sight(NLOS) case that the transmitter(Tx) is located on the corridor while the receiver(Rx) is moved along the corner and stair. The floor is marble and the ceiling is plaster at a height of 3.2 m. The stair step is made of reinforced concrete with width of 133 cm, length of 26 cm, and height of 16.5 cm. In order to obtain the transfer function of each link(H_{11}, H_{12}, H_{21}, H_{22}), Rx is moved on the prepared six locations(Rx6-Rx11) in the corner and stair as shown in Fig.2.

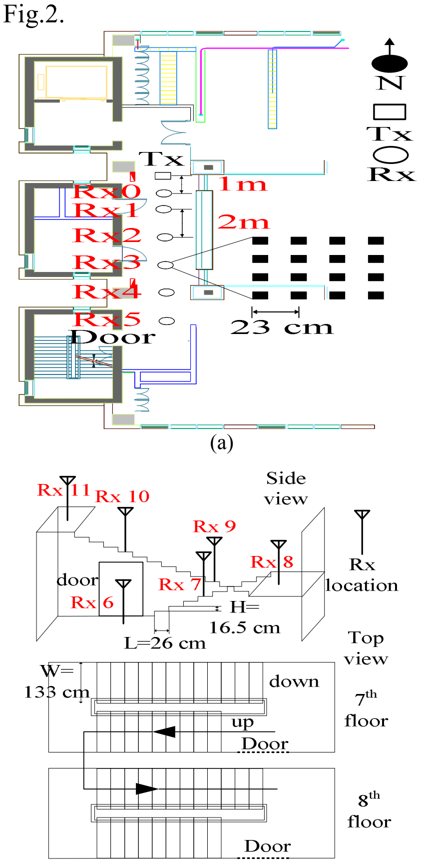

Figure 2: Layout of measurement environment: a) corridor, b) stairwell.

III. A Sigular Value Decomposition MIMO Channel Model

A. The MIMO Channel Impulse Response Matrix

For a MIMO system with two transmit antennas and two receive antennas, the relationship between transmitted and received signals can be expressed as

$$y = Hx + n \tag{1}$$

where y is the 2×1 received signal, x is 2×1 the transmitted signal and n is the noise. H is the 2×2 CIR matrix whose entry h_{mn} is the scalar valued frequency response between the nth transmit antenna and the mth receive antenna[12].

$$H = \begin{pmatrix} h_{11} & h_{12} \\ h_{21} & h_{22} \end{pmatrix} \tag{2}$$

For a Rician fading channel, the CIR matrix is given by

$$H = \sqrt{\frac{K}{K+1}} H_{LOS} + \sqrt{\frac{1}{K+1}} H_{res} \tag{3}$$

where H_{LOS} reflects the contribution of line of sight(LOS) componet and H_{res} reflects the residue stochastic part of CIR matrix. K is the Rician factor. This paper discusses the NLOS case only(Rx6-Rx11), then K=0. That is to say $H=H_{res}$ and corresponds to a Rayleigh fading case[12].

B. Singular Value Decomposition Model

Based on the singular value decomposition, a novel model is discussed in this part. According to singular value decomposition of matrix, the 2×2 CIR matrix H can be expressed as

$$H = U \Sigma V^H \tag{4}$$

$$\Sigma = \begin{pmatrix} \sigma_1 & 0 \\ 0 & \sigma_2 \end{pmatrix} \tag{5}$$

where σ_1, σ_2($\sigma_1 \geqslant \sigma_2 \geqslant 0$) are the sigular values of H, both U and V are unitary matrices.

We proposed that the unitary matrix U(V) can be divided into the determined part U_d(V_d) and the stochastic part U_s(V_s). That is to say, U, V can be expressed as

$$U = U_d \times U_s \tag{6}$$

$$V = V_d \times V_s \tag{7}$$

respectively. We difine that U_d(V_d) is the eigen-matrix of recei -ver(transmitter) and U_d(V_d) depends on the environment.

Equation (6) and (7) are substituted into (4) and then H can be modeled as

$$H = U_d U_s \begin{pmatrix} \sigma_1 & 0 \\ 0 & \sigma_2 \end{pmatrix} (V_d V_s)^H \tag{8}$$

C. Extractions of Model Parameters

In order to simplified model, we assume that U_s, V_s are any stochastic two dimension unitary matrices.

For any stochastic two dimension unitary, U_s, can be expressed as

$$U_s = \begin{pmatrix} a e^{j\omega_1} & \sqrt{1-a^2} e^{j\omega_2} \\ \sqrt{1-a^2} e^{j\omega_3} & a e^{j(\omega_2+\omega_3-\omega_1+\pi)} \end{pmatrix} \tag{9}$$

where a, ω_1, ω_2, ω_3 are real valued and j is the complex unit. We assume that a is uniform distributed at interval [0,1] and ω_1, ω_2, ω_3 are uniform distributed at interval [0, 2π]. The stochastic two dimension unitary V_s can be assumed as same as U_s

Futhermore, from (8), we can get

$$E_H(HH^H) = U_d \times \Lambda_1 \times U_d^H \quad (10)$$

$$E_H(H^H H) = V_d \times \Lambda_2 \times V_d^H \quad (11)$$

where ∧1, ∧2 are two diagonal matrices. Through eigen decomposition of matrix $E_H(HH^H)$, the eigen-matrix of receiver U_d can be extracted. The eigen-matrix of transmitter V_d can also be extracted as same as U_d.

As we know, the sigular values σ_1, σ_2 are square root of eigenvalues. In [13,14], Wonsop Kim has discovered that eigenvalues of H follow Gamma distribution and developed the model of eigenvalues about the correlation coefficient. From the model in [13,14], we can easily get the expectation and variance of eigenvalues and then determine the distribution of eigenvalues. That is to say, the sigular values σ1, σ2 can be determined easily.

IV. Model Validation

In order to evaluate the performance of the novel model presented in this paper, two metrics, the joint DoA-DoD-delay power spectrum and the channel capacity of the model are compared with those obtained from the measured channels.

A. Joint DoA-DoD Power Spectrum

The Joint DoA-DoD Power Spectrum can be expressed using the Bartlett beamformer[12,15]

$$P_{Bart} = (a_{Tx}(\theta_{Tx}) \otimes a_{Rx}(\theta_{Rx}))^H \times R_{WB} \times (a_{Tx}(\theta_{Tx}) \otimes a_{Rx}(\theta_{Rx})) \quad (12)$$

$$R_{WB} = E_H(vec(H)vec(H)^H) \quad (13)$$

where R_{WB} is the full-correlation matrix, $a_{Tx}(\theta_{Tx})$, and $a_{Rx}(\theta_{Rx})$ are normalized steering vectors at θ_{Tx}, θ_{Rx} respectively.

The computed DoA-DoD Power Spectrum can reflect the spatial and delay characteristics of the radio channel. In order to quantify the power spectrum differences, we use the Kullback-Leibler divergence(KLD) to describe the differences[16]. The KLD is defined as follows:

$$\gamma = \int_x\int_y \overline{P_1}(x,y)\log\frac{\overline{P_1}(x,y)}{\overline{P_2}(x,y)}dxdy \quad (14)$$

$$\overline{P_i}(x,y) = P_i(x,y) / \int_x\int_y P_i(x,y)dxdy \quad (15)$$

where $P_i(x,y)$ is the DoA-DoD Power Spectrum.

The KLDs from novel modeled APS to the measured APS can be calculated and the results are shown in TableⅠ. In this table, it can be seen that the KLDs between the measured APS and the novel model are very small.

B. Capacity

The ergodic capacity of MIMO channel with equally allocated transmit power $\overline{C}$ can be determined as[17]

$$C = \log_2 \det(I_2 + \frac{SNR}{2}HH^H) \quad (16)$$

$$\overline{C} = E_H(C) \quad (17)$$

where C is the channel capacity, I_2 is an 2×2 identify matrix, SNR is the receive signal power to noise power ratio.

TABLE Ⅰ

The KLDs Between Modeled And Measured Joint DoA-DoD Angular Power Spectrums

Loc.	KLD		
	0.5λ Spa.	1λ Spa.	2λ Spa.
Rx6	0.195	0.154	0.08
Rx7	0.01	0.01	0.019
Rx8	0.04	0.11	0.026
Rx9	0.007	0.017	0.013
Rx10	0.02	0.022	0.025
Rx11	0.01	0.014	0.011

The 10% outage capacity of MIMO channel C_{out} can be calculated as[17]

$$P(C \le C_{out}) = 10\% \quad (18)$$

The capacity error from models to measurement is defined as

$$Error(\%) = \frac{C_{model} - C_{mea}}{C_{mea}} \quad (19)$$

where C_{model} is the modeled capacity and C_{mea} is the measured capacity.

The evaluation SNR is selected as 10 dB.

The ergodic capacity and the 10% outage capacity obtained from the measured channels and the novel model are shown in Fig.3 and Fig.4. For comparision, the ergodic capacity and the 10% outage capacity of Kronecker model and Weichselberger model are also shown in Fig.3 and Fig.4. The ergodic capacity errors and the outage capacity errors from each model to measurement are shown in TableⅡ and Table Ⅲ. The averaging ergodic capacity errors from novel model, Weichselberger model and Kronecker model to measurement are 0.39%, 5.77%, and 4.15% respectively. The averaging outage capacity errors from novel model, Weichselberger model and Kronecker model to measurement are 2.92%, 12.38%, and 15.07% respectively. From the results, two conclusions can be obtained. First, the capacity error from kronecker model to measurenment in this paper is smaller than other paper (i.e, in[18]) because the rank of 2×2 channel matrix is very small. Finally, the most important conclusion is that analyzing the results, the novel model presented in this paper matches better to the measured data than other models.

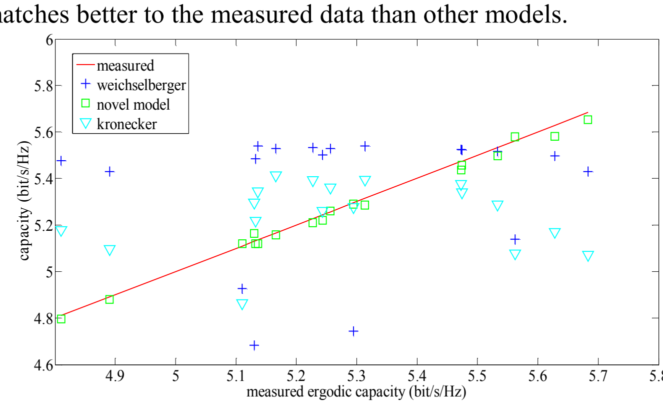

Figure 3: Ergodic capacity of every model and measured channels.

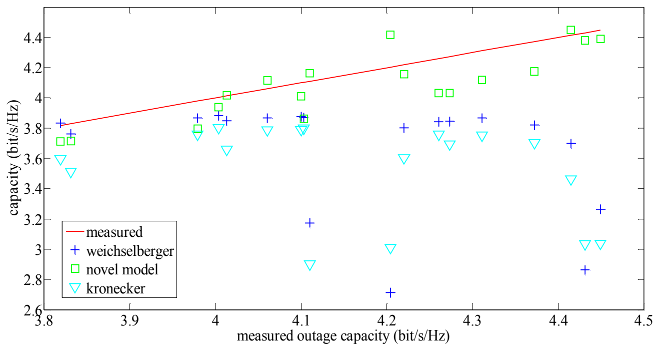

Figure 4: Outage capacity of every model and measured channels.

TABLE II
THE ERGODIC CAPACITY ERRORS FROM EACH MODEL TO MEASUREMENT

Loc. Spa.	Error(%)			Loc. Spa.	Error(%)		
	novel	web	kron		novel	web	kron
Rx6,0.5λ	0.1	10.4	0.3	Rx9,1λ	0.3	5.9	3.1
Rx7,0.5λ	0.7	1.0	1.8	Rx10,1λ	0.2	11.0	4.2
Rx8,0.5λ	0.5	4.5	10.8	Rx11,1λ	0.6	4.2	1.5
Rx9,0.5λ	0.1	5.2	2.0	Rx6,2λ	0.2	3.6	4.8
Rx10,0.5λ	0.3	13.8	7.6	Rx7,2λ	0.7	0.3	4.5
Rx11,0.5λ	0.3	7.8	4.0	Rx8,2λ	0.8	2.3	8.1
Rx6,1λ	0.7	8.7	3.2	Rx9,2λ	0.5	4.9	0.3
Rx7,1λ	0.3	1.0	2.4	Rx10,2λ	0.2	6.9	1.7
Rx8,1λ	0.3	7.63	8.7	Rx11,2λ	0.2	7.0	4.8

TABLE III
THE OUTAGE CAPACITY ERRORS FROM EACH MODEL TO MEASUREMENT

Loc. Spa.	Error(%)			Loc. Spa.	Error(%)		
	novel	web	kron		novel	web	kron
Rx6,0.5λ	5.1	35.5	28.5	Rx9,1λ	1.6	3.0	5.0
Rx7,0.5λ	1.4	4.7	6.8	Rx10,1λ	3.0	1.8	8.3
Rx8,0.5λ	0.8	16.2	21.5	Rx11,1λ	2.1	5.5	7.6
Rx9,0.5λ	5.4	9.8	11.8	Rx6,2λ	1.3	22.8	29.4
Rx10,0.5λ	2.8	0.4	5.8	Rx7,2λ	4.5	12.6	15.3
Rx11,0.5λ	4.6	2.8	5.5	Rx8,2λ	1.5	9.9	14.6
Rx6,1λ	1.1	35.4	31.6	Rx9,2λ	5.6	10.0	13.5
Rx7,1λ	4.4	10.3	13.0	Rx10,2λ	0.1	4.1	8.8
Rx8,1λ	1.3	26.6	31.7	Rx11,2λ	5.9	5.7	7.4

V. CONCLUSION

In this paper, a corridor to stair MIMO measurement at 2.6GHz is carried out. A novel MIMO model based on singular value decomposition of matrix is proposed in this paper. The joint DoA-DoD-delay power spectrum and the channel capacity are selected as two metrics to evaluate the performance of the novel model. The results show that the novel model provides a better fit to the measured data than Kronecker model and Weichselberger model. However, the frequency selectivity of channel are not considered in this novel model. Wider frequency bands are needed to achieve higher throughput in future wireless communication systems. An extension of the novel model adapted to wideband cases may be an important work in the next period.

ACKNOWLEDGEMENT

This work is supported by China Telecommunication Technology Labs(CTTL). Thanks to Yan Qin, Xiao-lei Wang and other employees in CTTL. Thanks to the teachers in Jiangsu Key Laboratory of Wireless Communications

REFERENCES

[1]. S. Sesia, I.Toufik, M.Baker, LTE-The UMTS Long Term Evolution From Theory to Practice. John Wiley & Sons, 2009
[2]. P. Almers, E.Bonek, and A. Burr et al., “Survey of channel and radio propagation models for wireless MIMO systems,” EURASIP J. Wireless Commun. New., vol. 2007, 2007, 10.1155/2007/19070, Article ID 19070.
[3]. H. Özcelik, “Indoor MIMO channel models,” Ph.D. dissertation, Institut für Nachrichtentechnik und Hochfrequenztechnik, Technische Universität Wien, Vienna, Austria, Dec. 2004
[4]. A. M. Saleh, R. R. Valenzuela, “A statistical model for indoor multipath propagation,” IEEE J. Sel. Areas Commun., vol. 52, no. 1, pp. 128-137, Feb. 1987.
[5]. Alighanbari, C. D. Sarris, “Parallel Time-Domain Full-Wave Analysis and System-Level Modeling of Ultrawideband Indoor Communication Systems,” IEEE Trans. Antennas Propag., vol. 57, no. 1, pp. 231-240, JAN. 2009
[6]. T. Zwick, C. Fischer, W. Wiesbeck, “A stochastic multipath channel model including path directions for indoor environments,” IEEE J. Sel. Areas Commun., vol. 20, no. 6, pp. 1178-1192, Aug.2002.
[7]. P. Petrus, J. H. Reed, T. S. Rappaport, “Geometrical-based statistical mcrocell channel model for mobile environment,” IEEE Trans. Commun., vol. 50, no. 3, pp. 495-502, Mar. 2002
[8]. J. P. Kermoal, L. Schumacher, K. I. Pedersen, P. E. Mogensen, F. Frederiksen, “A stochastic MIMO radio channel model with experimental validation,” IEEE J. Sel. Areas Commun, vol. 20, pp. 1211–1226, Aug. 2002.
[9]. W. Weichselberger, M. Herdin, H. Özcelik, E. Bonek, “A stochastic MIMO channel model with joint correlation of both link ends,” IEEE Trans. Wireless Commun., vol. 5, pp. 90–100, Jan. 2006.
[10]. M. Sayeed, “Deconstructing multiantenna fading channels,” IEEE Trans. Signal Process., vol.50, pp. 2563-2579, Oct. 2002.
[11]. R. Vaughan, J. B. Andersen, Channels, Antennas, and Propagation for Mobile Communications. London, U. K. : IEE, 2003.
[12]. Y. Zhang, O. Edfors, P. Hammarberg, et al., “A General Coupling Based Model Framework for Wideband MIMO Channels,” IEEE Trans. Antennas Propag., vol. 60, no. 2, pp. 574-586, Feb. 2012
[13]. W. Kim, K. Lee, M. D. Kim, J. J. Park, H. K. Chung, H. Lee, “Performance analysis of spatially correlated MIMO-OFDM beamforming systems with the maximum eigenvalue model from measured MIMO channels,” IEEE Trans. Wireless Commun., vol. 11, pp. 3744-3753, Oct. 2012.
[14]. W. Kim, K. Lee, M. D. Kim, J. J. Park, H. K. Chung, “Distribution of Eigenvalues for 2×2 MIMO Channel Capacity Based on Indoor Measurements,” IEEE Trans. Wire. Commun., vol. 11, no. 4, pp. 1255-1259, Apr. 2012.
[15]. W. Weichselberger, “Spatial structure of multiple antenna radio channels,” Ph.D. dissertation, Vienna Univ. of Technology, Vienna, Austria, 2003
[16]. T. T. Georgiou, “Distances and Riemannian metrics for spectral density functions,” IEEE Trans. Signal Process., vol. 55, no. 8, pp. 3995-4003, Aug. 2007
[17]. J. G. Proakis, Digtial Communications, 3rd ed. New York: McGraw-Hill, 1995
[18]. S. Wyne, A. F. Molisch, P. Almers, et al., “Outdoor-to-Indoor Office MIMO Measurements and Analysis at 5.2 GHz,” IEEE Trans Veh. Technol., vol. 57, no. 3, pp. 1374-1386, Ma -y 2008.